



Black Start by HVdc-connected Offshore Wind Power Plants

Sakamuri, Jayachandra Naidu; Göksu, Ömer; Bidadfar, Ali; Saborío-Romano, Oscar; Jain, Anubhav; Cutululis, Nicolaos Antonio

Published in:
Proceedings of the IEEE 45th Annual Conference of the Industrial Electronics Society

Link to article, DOI:
[10.1109/IECON.2019.8927615](https://doi.org/10.1109/IECON.2019.8927615)

Publication date:
2019

Document Version
Peer reviewed version

[Link back to DTU Orbit](#)

Citation (APA):
Sakamuri, J. N., Göksu, Ö., Bidadfar, A., Saborío-Romano, O., Jain, A., & Cutululis, N. A. (2019). Black Start by HVdc-connected Offshore Wind Power Plants. In *Proceedings of the IEEE 45th Annual Conference of the Industrial Electronics Society* (pp. 7045-7050). IEEE. <https://doi.org/10.1109/IECON.2019.8927615>

General rights

Copyright and moral rights for the publications made accessible in the public portal are retained by the authors and/or other copyright owners and it is a condition of accessing publications that users recognise and abide by the legal requirements associated with these rights.

- Users may download and print one copy of any publication from the public portal for the purpose of private study or research.
- You may not further distribute the material or use it for any profit-making activity or commercial gain
- You may freely distribute the URL identifying the publication in the public portal

If you believe that this document breaches copyright please contact us providing details, and we will remove access to the work immediately and investigate your claim.

Black Start by HVdc-connected Offshore Wind Power Plants

Jayachandra N. Sakamuri, Ömer Göksu, Ali Bidadfar, Oscar Saborío-Romano, Anubhav Jain, Nicolaos A. Cutululis
DTU Wind Energy, Technical University of Denmark
Roskilde, Denmark

Abstract— The current practice of power system restoration mainly relies on conventional power plants, which can provide black start in case of a black out using fossil fuels. HVdc-connected offshore wind power plants can, on the other hand, provide fast and environmentally friendly solutions for power system restoration, once their state of the art wind turbines are equipped with the grid-forming capability. In this paper, the background and existing solutions for wind turbine and wind power plant self-energization and onshore grid black start are presented, together with simulation results of an offshore wind power plant sequentially energizing the offshore ac network, offshore HVdc terminal, HVdc link, onshore HVdc terminal, and onshore ac terminal and load.

Black start, energization, grid-forming wind turbine control, HVdc transmission, offshore wind energy integration

I. INTRODUCTION

In HVdc-connected offshore wind power plants (OWPPs), the current practice for energization of the offshore ac network between the offshore HVdc converter and the wind turbines (WTs) relies on the black-start (grid-forming) capability of the offshore HVdc terminal, taking the necessary energy from the onshore ac network via the HVdc link. Hence, in case of a long-lasting electricity shortage due to the outage of the HVdc link or an onshore black out, other auxiliary power supplies are needed for supplying the WT auxiliary loads [1],[2]. This requires either permanently installed diesel generators at the offshore HVdc platform or temporary mobile diesel generators being carried to the offshore site, which both increases the operational and insurance costs and decreases reliability due to diesel generator issues. Similarly, diesel generators are needed for the supply of auxiliary units in the offshore HVdc platform (e.g. controls, switchgear, air-conditioning units).

State of the art (type-4) WTs with fully rated power electronics converters can be controlled to function so that they can start and operate without the need for external auxiliary power supplies (grid-forming/black-start-able WTs [3]). By means of such capabilities, such WTs can form the offshore ac network, i.e. control its voltage magnitude and frequency, for as long as the wind allows [1] [2]. The capability of energizing their offshore ac network both for short and long periods of time can help reduce the current need for auxiliary diesel generators. Moreover, it can provide cost-effective,

fast and environmentally friendly alternatives for offshore ac network energization, onshore ac network black start and power system restoration in general.

The current practice of power system restoration mainly relies on conventional power plants, which can provide black start in case of a black out. The black-start capability of conventional power plants, which requires auxiliary units to start up and generate the onshore ac network voltage, is characterized by long start-up times due to their slow (for instance thermal) dynamics, and extended use of fossil fuels to keep them ready for service. OWPPs can, on the other hand, provide fast and environmentally friendly solutions for power system restoration, once their state of the art WTs are equipped with the black-start capability. *Black start* and *island operation* have been included in ENTSO-E's network connection requirements (*RfG* and *HVDC*) as optional requirements for (both ac- and HVdc-connected) WPPs, which can be requested by the TSOs [4], [5]. Moreover, there is an increasing interest from TSOs to have black-start capabilities from the HVdc networks connected to their ac networks [6]-[9], which implies that the HVdc converters be designed for electrical transients during onshore ac network black start. Black start by HVdc-connected OWPPs has been studied so far in [10]–[12]. Such works, however, have not studied the HVdc converter energization in detail, which is the aim of the present study. The method presented in [11] is applied in [10] to island operation of HVdc-connected offshore WTs and onshore black start, analyzing the WT mechanical loads during such scenarios. It is assumed that an external generator provides auxiliary power to the WPP. In [13], frequency control methods of an ac-connected WPP are evaluated when the WPP is employed for black start of a regional grid, with a diesel generator providing auxiliary power.

In the present study, control schemes for grid-forming WTs and HVdc converters are presented together with simulation results of an OWPP sequentially energizing the offshore ac network, offshore HVdc terminal, HVdc link, onshore HVdc terminal, and onshore ac terminal and load. The rest of the paper is organized as follows. The considered system model is presented in Section II. In Section III, simulation results are presented and discussed. Finally, concluding remarks are given in Section IV.

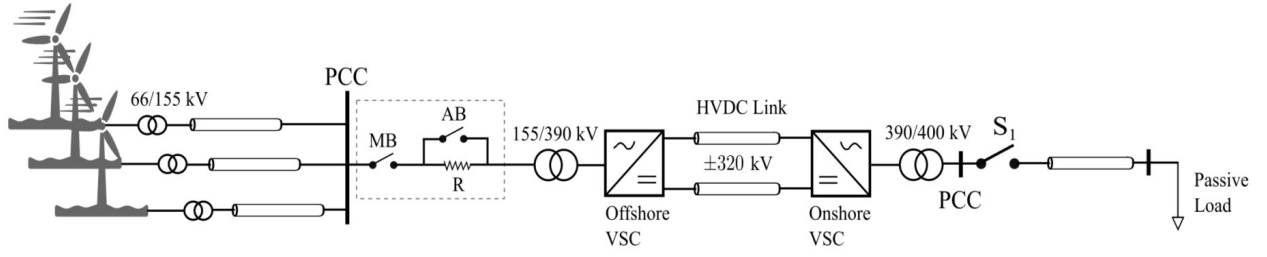


Figure 1. Schematic of HVdc-connected offshore wind power plant energizing a passive load.

II. SYSTEM MODEL

In this section, the considered system model, shown in Figure 1, is briefly described. A symmetrical monopole configuration is used for the HVdc connection. The main circuit parameters are given in Table I. Each HVdc terminal uses half-bridge modular multi-level converters (MMCs). The fundamental structure of an MMC is shown in Figure 2, together with important measurements, such as voltage at the point of common coupling, U_{pcc} , converter ac terminal voltage and current, U_c and i_c , respectively, valve currents i_v , cell voltage, U_{cell} , and terminal dc voltage, U_{dc-pn} . The active and reactive powers are measured at the PCCs. The HVdc converter consists of six arms, each having n sub-modules (SMs) connected in series.

The offshore HVdc converter uses grid-following controls, oriented on to the offshore ac network voltage formed by the WPP. By means of such controls, the converter regulates the voltage on its dc terminals and its reactive power output to the offshore ac network. The converter has standard half-bridge MMC inner control loops, such as cell voltage balancing control and circulating current controls. The block diagram of the converter outer control loops is shown in Figure 3, where PLL, CC, and PI stand for phase-locked loop, current controller, and proportional-integral (controller), respectively. The letters shown in bold represent the vector variables in the rotating (dq) reference frame, oriented on the converter ac terminal voltage.

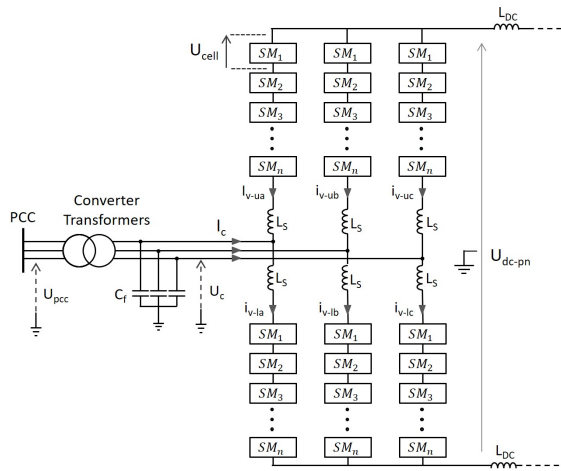


Figure 2. Half-bridge MMC topology

TABLE I. HVDC MAIN CIRCUIT PARAMETERS

Parameters	Values
WPP rating	1000 MW (400, 400, 200)
WT rating	8 MW, 66 kV
WPP trasformer rating	66/155 kV, 415 MVA, 210 MVA
HVdc converter	1050 MVA, 10% reactance
HVdc transformers	155/390 kV (Offshore), 400/390 kV (Onshore), 12% reactance
MMC	Half-bridge, ($n =$) 225 submodules
HVdc link voltage	± 320 kV

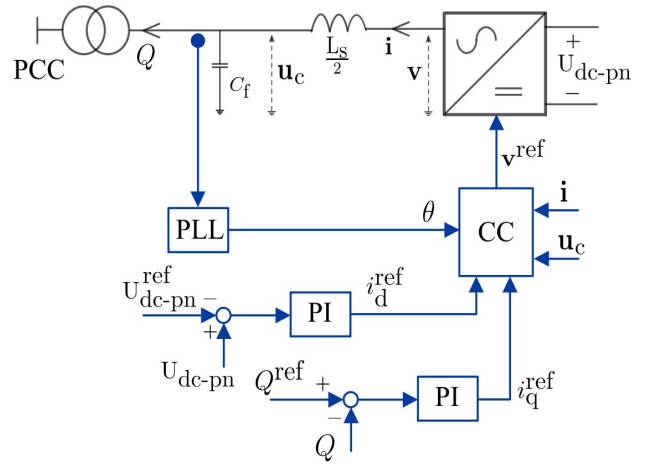


Figure 3. Offshore HVdc converter control

The onshore HVdc converter operates as a grid-forming converter, meaning that it controls the ac network voltage magnitude and frequency. Since there is only one converter feeding the passive ac system, the frequency reference is kept constant. The block diagram of the corresponding controls is shown in Figure 4. The vector variables are represented in a rotating (dq) reference frame with angular speed given by the frequency reference.

A 1000 MW WPP cluster having two 400 MW WPPs and one 200 MW WPP is considered for this study. Each 400 MW WPP has 50 8 MW WTs, whereas the 200 MW WPP has 25 8 MW WTs. One 400 MW WPP is active for the considered case. The WTs use fully-rated converters to

connect to the offshore ac network. The WT back-end (generator-side) converters control the WT dc link voltage, whereas the WT front-end (grid-side) converters operate as grid-forming units, i.e. they control the magnitude and frequency of their ac terminal voltage.

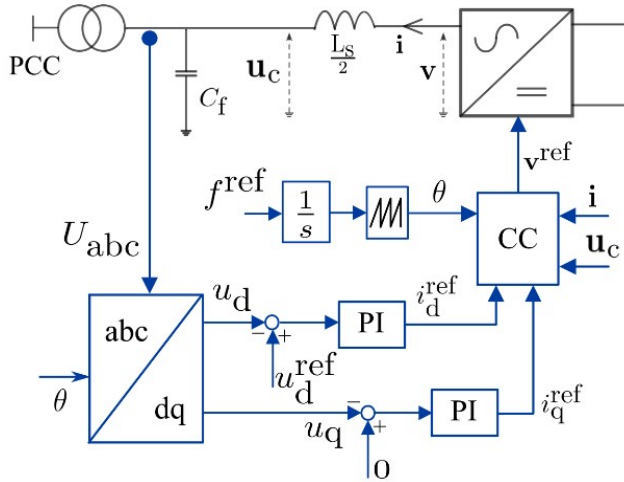


Figure 4. Onshore HVdc converter control

A WT front-end converter (FEC) and corresponding grid-forming controls are shown in Figure 5. The control scheme, based on those in [14], [15], uses a distributed phase-locked-loop-based frequency control, implemented for each WT front-end converter in a rotating reference frame oriented on the converter ac terminal voltage \mathbf{u}_c . In such scheme, each grid-forming WT FEC controls its ac terminal voltage (magnitude) and frequency.

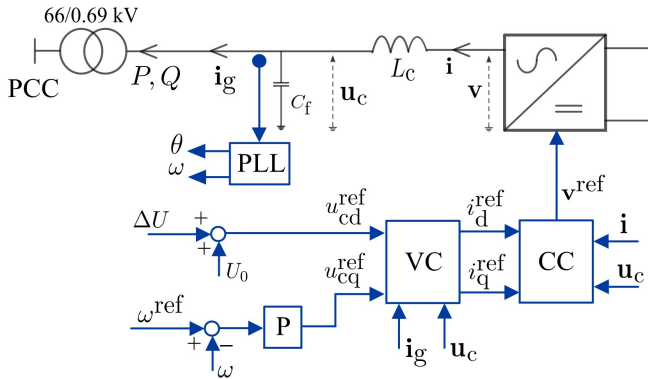


Figure 5. Wind Turbine Front-End Converter Control

III. SIMULATION RESULTS

In this section, the energization sequence, summarized in Table II, is described in detail. The stages of the energization sequence can be understood by referring to Figure 1.

TABLE II. ENERGIZATION SEQUENCE

Stage	Time [s]	Events (refer Figure 1)
1	< 0	WPP energized
2	1.3	ac circuit breaker [MB] closed
	1.6	Pre-insertion-resistor (PIR) bypassed by closing the circuit breaker [AB]
	2.1	offshore HVdc converter deblocked; HVdc link energized
3	2.75	onshore HVdc converter deblocked; onshore ac terminal energized
4	4	onshore load connected

The energization of the WPP with the grid-forming control of WTs is explained in [14] and [15], therefore, the rest of the energization sequence is explained in this paper. Therefore, the impact on the PCC voltage, converter ac terminal voltage, valve currents, cell voltage, dc terminal voltage and active and reactive powers at each converter is presented.

Stage 2: offshore HVdc converter energization

The responses of the offshore and onshore HVdc converters are shown in Figures 6 and 7, respectively. Once the offshore HVdc converter ac breaker (MB in Figure 1) is closed at $t = 1.3$ s, the converter is charged through the PIR in a controlled (limited transients) manner; thus protecting the wind turbines and valves from transient overcurrent due to the energization of the transformer (magnetizing inrush current). Moreover, the controlled ramp in the converter voltage limits the charging current of the MMC submodule capacitors.

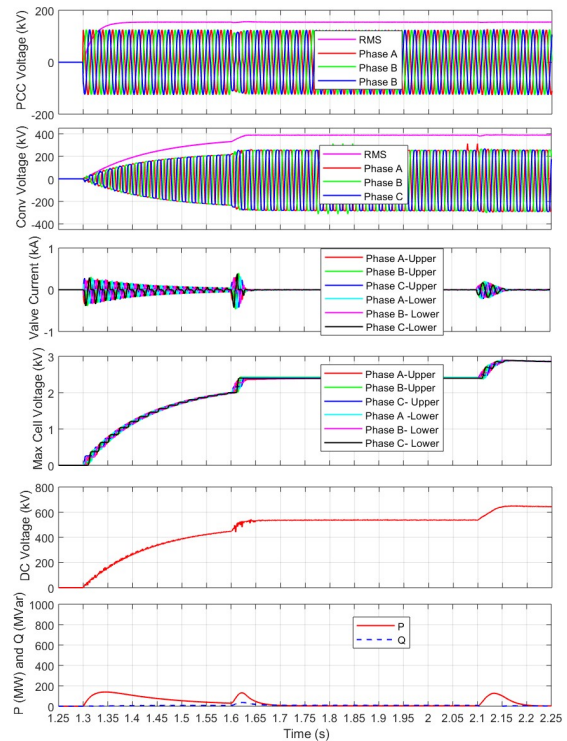


Figure 6. Offshore HVdc converter response – stage 2

Once the submodules are charged to around 2 kV, the PIR is bypassed (By closing the AB in figure 1) at $t = 1.6$ s, allowing faster charging. Sudden increases in the converter

ac terminal voltage, valve currents, maximum cell voltage, and dc terminal voltage can be observed. The magnitude of such increases is, however, well within the acceptable levels.

Once the offshore HVdc converter is deblocked at $t = 2.1$ s, the HVdc link voltage is increased to 640 kV. The maximum cell voltage is around 2.85 kV, which is well below the limits (4 kV). It is clear that the impact is mainly at offshore HVdc converter. The onshore HVdc converter submodules are charged to 1.45 kV (half of the offshore HVdc converter cell voltage). The reason is that the 450 submodules between the two valve arms (225 in each arm) share the HVdc link voltage (640 kV). The WPP ac terminal voltage and active and reactive power outputs during stage 2 are shown in Figure. 8. Apart from minor transients in the terminal ac voltage, there is no significant transients observed.

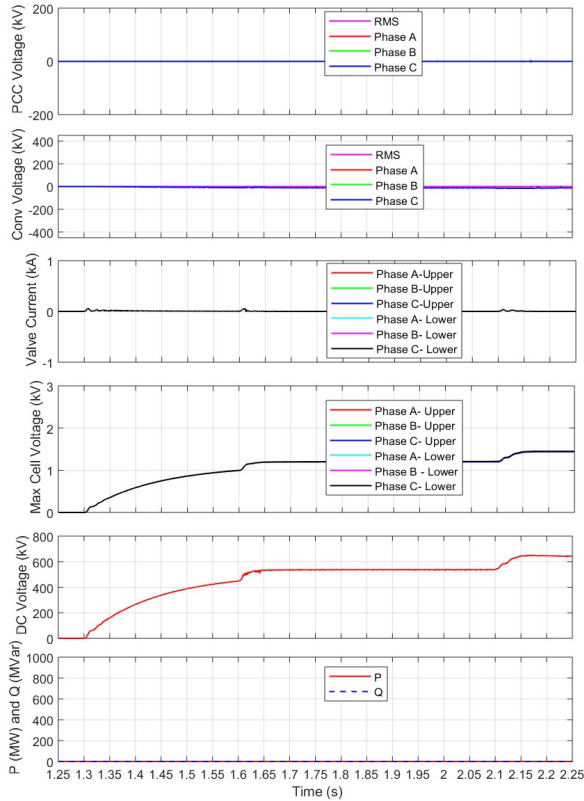


Figure 7. Onshore HVdc converter response – stage 2

Stage 3: onshore ac network energization

The grid-forming onshore HVdc converter is deblocked at $t = 2.75$ s. As shown in Figures 9 (onshore) and 10 (offshore), the onshore HVdc converter submodules start charging once the converter is deblocked and reach the desired cell voltage (2.85 kV) within 300 ms. At the same time, the onshore HVdc converter starts forming the ac voltage at its terminals. A dip in the HVdc link voltage and disturbance in the offshore converter submodule cell voltages can be observed during the charging process. It is due to the energy imbalance in the dc system. The submodule capacitors in the offshore HVdc converters discharge during the charging of submodules of onshore HVdc converter. The WPP then reacts to the energy imbalance by producing the required active power for charging the onshore converter and form-

ing the onshore ac network. The HVdc system settles within 300 ms and the onshore converter controls the onshore ac network voltage to its desired magnitude (400 kV) and frequency (50 Hz).

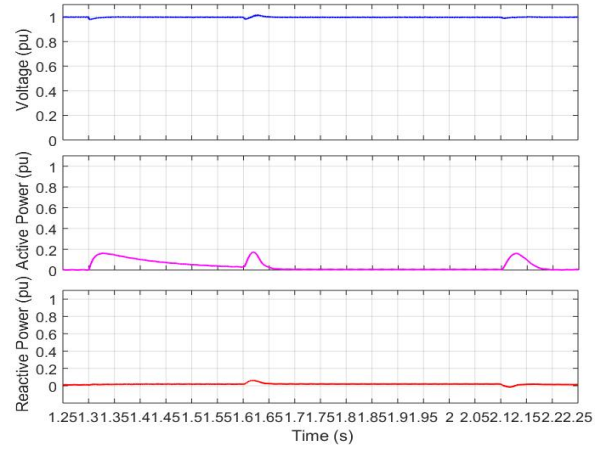


Figure 8. WPP response – stage 2

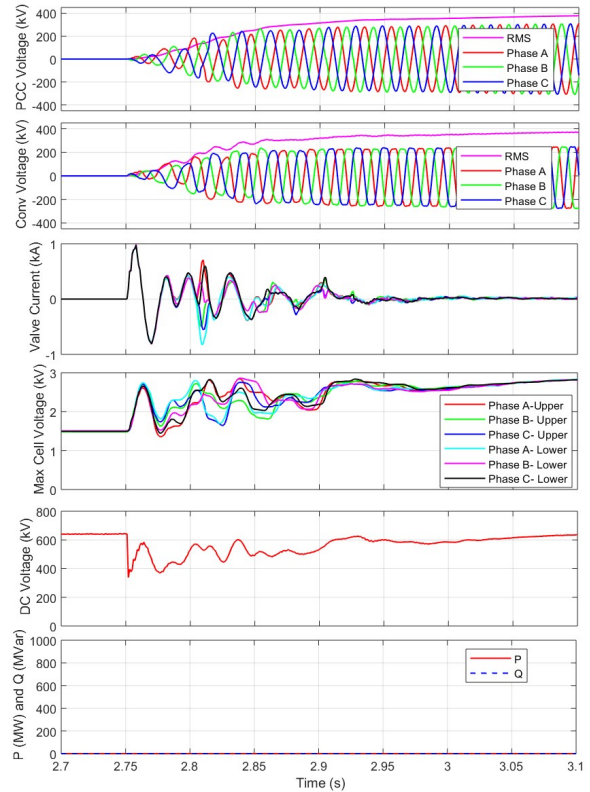


Figure 9. Onshore HVdc converter response – stage 3

Stage 4: Onshore load connection

Once the onshore ac network voltage is established, an active power load of 400 MW is connected to it at $t = 4$ s. The corresponding onshore and offshore HVdc converter responses are shown in Figures 11 and 12, respectively. A small dip (5 %) is briefly observed in the HVdc link voltage, which recovers quickly once the offshore HVdc converter and WPP start supplying the required active power to the onshore ac network. The PCC voltage, converter bus volt-

age, valve currents, cell voltages well within limits, both at onshore and offshore converters, for a step change in active power at onshore AC terminal.

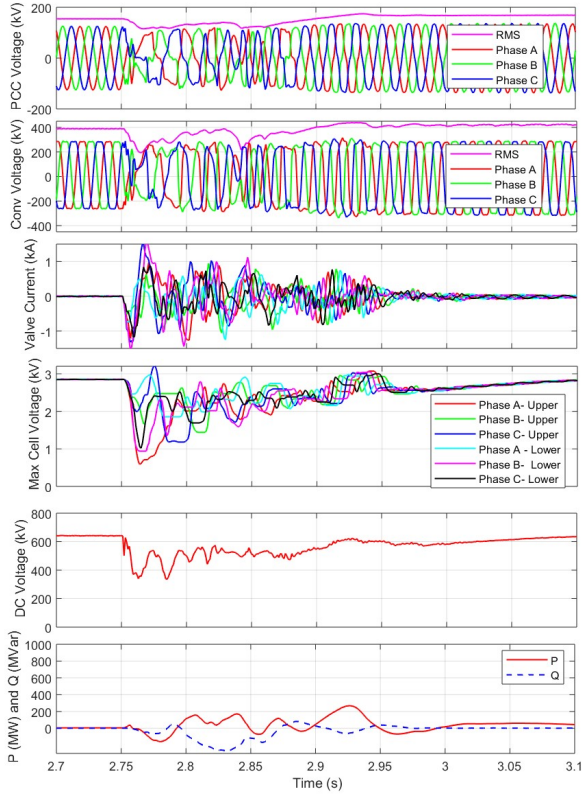


Figure 10. Offshore HVdc converter response – stage 3

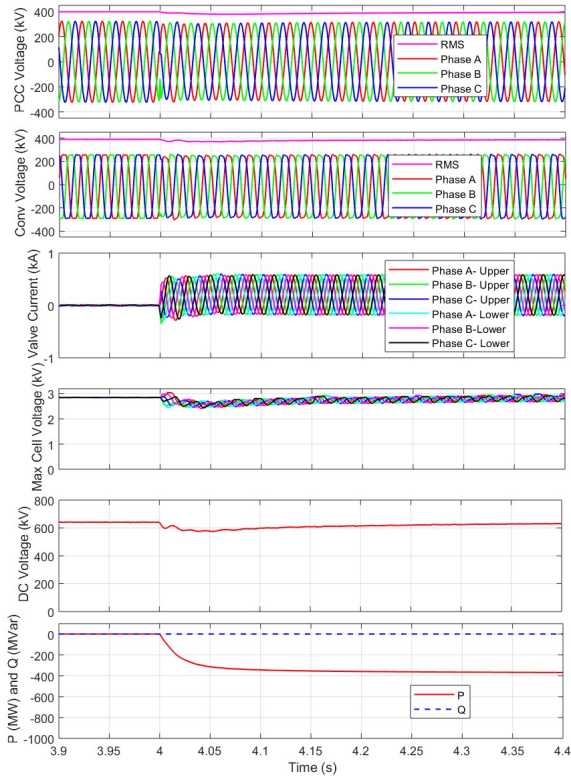


Figure 11. Onshore HVdc converter response – stage 4

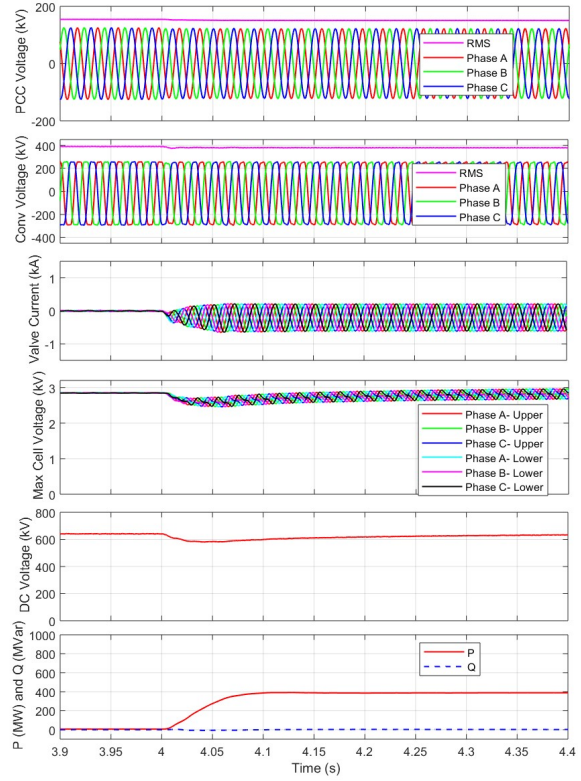


Figure 12. Offshore HVdc converter response – stage 4

IV. CONCLUSION

In this paper, the energization of an onshore ac network by OWPPs connected through an HVdc link has been explained. The simulation results have shown that the grid-forming capabilities of WTs can be used to establish the offshore ac voltage and thereafter energize the offshore HVdc converter, HVdc link, and onshore HVdc converter. The pre-insertion resistor connected at the offshore HVdc converter ac terminals helps protect the WTs against large inrush currents and control the charging of the HVdc converter submodules.

It is shown that HVdc-connected OWPPs using the modern fast-responding WTs can behave as black-start units in the restoration of future power systems with high shares of converter-interfaced energy resources. The use of WPPs as black-start units would require adapting the market for this purpose, e.g. considering the wind speed forecast in the restoration process. Moreover, it is important to study the impact on the MMC HVdc system of energizing the onshore ac network by means of the grid-forming offshore WPPs.

ACKNOWLEDGEMENT

This work has received funding from the European Union's Horizon 2020 research and innovation programme under grant agreement No 691714.

REFERENCES

- [1] Ö. Göksu, O. Saborío-Romano, N. A. Cutululis, and P. Sørensen, "Black Start and Island Operation Capabilities of Wind Power Plants," in *Proceedings of the 16th Wind Integration Workshop*, Berlin, Germany, 25th–27th Oct. 2017. Available: https://www.promotion-offshore.net/fileadmin/PDFs/Conference_Paper_Black_

- Start and Island Operation Capabilities of Wind Power Plants with note.pdf.
- [2] A. Jain, K. Das, Ö. Göksu, and N. A. Cutululis, "Control Solutions for Blackstart Capability and Islanding Operation of Offshore Wind Power Plants," in *Proceedings of the 17th Wind Integration Workshop*, Stockholm, Sweden, 17th–19th Oct. 2018. Available: http://orbit.dtu.dk/files/158921420/WIW18_097_posterpaper_Anubhav_Jain.pdf.
 - [3] Huw Williams, "Offshore Wind Accelerator - R&D gaps in offshore wind," presented at the *NORCOWE 2016 Conference*, Bergen, Norway, 14th–16th Sep. 2016. Available: <http://www.norcowe.no/doc/konferanser/2016/NORCOWE%202016%20presentations/Future%20OSW%20R&D%20gaps%20-%20Huw%20Williams%20-%20Carbon%20Trust.pdf>.
 - [4] ENTSO-E, "Network code on requirements for grid connection of high voltage direct current systems and direct current-connected power park modules," Brussels, Belgium, Network Code, Aug. 2016. Available: <http://eur-lex.europa.eu/legal-content/EN/TXT/PDF/?uri=CELEX:32016R1447&from=EN>.
 - [5] —, "Network code on requirements for grid connection of generators," Brussels, Belgium, Network Code, Apr. 2016. Available: <http://eur-lex.europa.eu/legal-content/EN/TXT/PDF/?uri=CELEX:32016R0631&from=EN>.
 - [6] M. Bahrman and P.E. Bjorklund, "The New Black Start: System Restoration with Help from Voltage-Sourced Converters," *IEEE Power and Energy Magazine*, vol. 12, no. 1, pp. 44–53, Jan.–Feb. 2014.
 - [7] J. P. Kjærgaard, "The Skagerrak4 project – Connecting renewables with new technology between Denmark and Norway," presented at the *EPE Joint Wind Energy and T&D Chapters Seminar*, Aalborg, Denmark, 28th–29th Jun. 2012. Available: <http://www.epe-association.org/epe/seminars/Wind2012/Keynotes/WECS%202012%20-%20Keynotes%20-%202012-6-2012.pdf>.
 - [8] D. van Hertem, O. Gomis-Bellmunt, and J. Liang, Eds., *HVDC Grids: For Offshore and Supergrid of the Future*. Hoboken, NJ, United States: John Wiley & Sons, Mar. 2016.
 - [9] T. Midtsund, A. Becker, J. Karlsson, and K.A. Egeland, "A Live Black-start Capability test of a Voltage Source HVDC Converter," in *Proceedings of the 2015 CIGRÉ Canada Conference*, Winnipeg, MB, Canada, 31st Aug. – 2nd Dec. 2015.
 - [10] E.F. Belenguer-Balaguer, R. Vidal-Albalade, H. Beltrán-San-Segundo, and R.M. Blasco-Giménez, "Control Strategy for Islanded Operation of Offshore Wind Power Plants Connected through a VSC-HVDC," in *Proceedings of the IEEE IES 39th Annual Conference (IECON 2013)*, Vienna, Austria, 10th–13th Nov. 2013, pp. 5254–5259.
 - [11] E.F. Belenguer-Balaguer, R. Vidal-Albalade, H. Beltrán-San-Segundo, R.M. Blasco-Giménez, "Analysis of Control Alternatives for Offshore Wind Farms Connected through a VSC-HVDC Link", in *Proceedings of the 11th Wind Integration Workshop*, Lisbon, Portugal, 13th–15th Nov. 2012.
 - [12] H. Becker, A. Naranovich, T. Hennig, A. Akbulut, D. Mende, S. Stock, and L. Hofmann, "System Restoration using VSC-HVDC connected Offshore Wind Power Plant as Black-Start Unit," in *Proceedings of the 19th European Conference on Power Electronics and Applications (EPE 2017 – ECCE Europe)*, Warsaw, Poland, 11th–14th Sep. 2017.
 - [13] Y. Tang, J. Dai, Q. Wang, and Y. Feng, "Frequency Control Strategy for Black Starts via PMSG-Based Wind Power Generation," *Energies*, vol. 10, no. 3, Mar. 2017.
 - [14] L. Yu, R. Li, and L. Xu, "Distributed PLL-Based Control of Offshore Wind Turbines Connected With Diode-Rectifier-Based HVdc Systems," *IEEE Transactions on Power Delivery*, vol. 33, no. 3, pp. 1328–1336, Jun. 2018.
 - [15] O. Saborío-Romano, A. Bidafar, J. N. Sakamuri, Ö. Göksu, and N. A. Cutululis, "Primary Frequency Response from Offshore Wind Farms Connected to HVdc via Diode Rectifiers," in *Proceeding of the IEEE PES 13th PowerTech Conference*, Milan, Italy, 23rd–27th Jun. 2019.